

ORIGINAL ARTICLE

Hapten-derivatized nanoparticle targeting and imaging of gene expression by multimodality imaging systems

C-M Cheng¹, P-Y Chu², K-H Chuang¹, SR Roffler³, C-H Kao¹, W-L Tseng^{4,5}, J Shiea^{4,5}, W-D Chang⁶, Y-C Su⁶, B-M Chen³, Y-M Wang^{7,8} and T-L Cheng^{5,6,8}

¹Graduate Institute of Medicine, Kaohsiung Medical University, Kaohsiung, Taiwan; ²Faculty of Biomedical Laboratory Science, Kaohsiung Medical University, Kaohsiung, Taiwan; ³Institute of Biomedical Sciences, Academia Sinica, Taipei, Taiwan; ⁴Department of Chemistry, National Sun Yat-sen University, Kaohsiung, Taiwan; ⁵National Sun Yat-Sen University-Kaohsiung Medical University Joint Research Center, Kaohsiung, Taiwan; ⁶Faculty of Biomedical Science and Environmental Biology, Kaohsiung Medical University, Kaohsiung, Taiwan and ⁷Faculty of Medicinal and Applied Chemistry, Kaohsiung Medical University, Kaohsiung, Taiwan

Non-invasive gene monitoring is important for most gene therapy applications to ensure selective gene transfer to specific cells or tissues. We developed a non-invasive imaging system to assess the location and persistence of gene expression by anchoring an anti-dansyl (DNS) single-chain antibody (DNS receptor) on the cell surface to trap DNS-derivatized imaging probes. DNS hapten was covalently attached to cross-linked iron oxide (CLIO) to form a 39 ± 0.5 nm DNS-CLIO nanoparticle imaging probe. DNS-CLIO specifically bound to DNS receptors but not to a control single-chain antibody receptor. DNS-CLIO (100 μ m Fe) was non-toxic to both B16/DNS (DNS receptor positive) and B16/phOx (control receptor positive) cells. Magnetic resonance (MR) imaging could detect as few as 10% B16/DNS cells in a mixture *in vitro*. Importantly, DNS-CLIO specifically bound to a B16/DNS tumor, which markedly reduced signal intensity. Similar results were also shown with DNS quantum dots, which specifically targeted CT26/DNS cells but not control CT26/phOx cells both *in vitro* and *in vivo*. These results demonstrate that DNS nanoparticles can systemically monitor the expression of DNS receptor *in vivo* by feasible imaging systems. This targeting strategy may provide a valuable tool to estimate the efficacy and specificity of different gene delivery systems and optimize gene therapy protocols in the clinic.

Cancer Gene Therapy (2009) **16**, 83–90; doi:10.1038/cgt.2008.50; published online 19 September 2008

Keywords: non-invasive imaging; anti-dansyl (DNS); single-chain antibody; DNS-derivatized imaging probes; DNS-CLIO nanoparticle; DNS-quantum dots; gene delivery system

Introduction

Non-invasive imaging of gene expression is important for both current and future clinical gene therapy trials, allowing definition of the location, magnitude and persistence of gene expression. Several systems are being developed to trace gene expression, including nuclear imaging (gamma camera and positron emission tomography),^{1,2} magnetic resonance (MR) imaging^{3,4} and optical imaging

of live animals.^{5,6} Nuclear imaging modalities are characterized by high sensitivity, but suffer from poor spatial and temporal resolution.⁷ Optical imaging is relatively inexpensive and robust but clinical applications are hindered by limited depth penetration.⁸ MR imaging techniques provide spectacular resolution and can measure more than one physiological parameter by using different frequency pulse sequences,⁹ but imaging sensitivity is inferior to nuclear techniques.¹⁰ Thus, each imaging system has pros and cons for biomedical research.

Development of multimodality imaging protocols can help overcome limitations of single imaging modalities for *in vivo* assessment of molecular processes. We previously reported a novel gene/probe imaging system based on the expression of anti-DNS (5-dimethylamino-1-naphthalene sulfonic acid) single-chain antibody receptors (DNS receptor) on cells to trap DNS-derivatized imaging probes to assess the location, extent and persistence of gene expression in live animals.¹¹ We showed that a bivalent (DNS)₂-diethylenetriaminepentaacetate-¹¹¹Indium ((DNS)₂-DTPA-¹¹¹In) probe could specifically localize to

Correspondence: Dr T-L Cheng, Faculty of Biomedical and Environmental Biology, Kaohsiung Medical University, 100 Shih-Chuan 1st Road, Kaohsiung, Taiwan.

E-mail: tlcheng@kmu.edu.tw

Dr Y-M Wang, Faculty of Medicinal and Applied Chemistry, Kaohsiung Medical University, 100 Shih-Chuan 1st Road, Kaohsiung, Taiwan.

E-mail: m825010@kmu.edu.tw

⁸These authors contributed equally to this work.

Received 27 August 2007; revised 3 December 2007; accepted 10 January 2008; published online 19 September 2008

DNS receptors on B16/F1 tumors in mice as assessed by gamma camera imaging.¹¹ However, an analogous gadolinium probe ((DNS)₂-DTPA-Gd (III)) could not be detected by MR imaging due to poor sensitivity (unpublished results). Recently, non-toxic cross-linked iron oxide (CLIO) superparamagnetic nanoparticles have been developed as an excellent MR signal enhancer to resolve a major weakness of current MR imaging techniques for gene expression^{12,13} and cell tracking^{14,15} *in vivo*. In addition, quantum dots (qdots), fluorescent nanoparticles with improved signal intensity and resistance against photobleaching, have also been extensively used for sensitive imaging of cells and animals,^{16–18} thus revitalizing traditional fluorescence imaging methodologies.¹⁹ Based on these results, we hypothesized that covalent conjugation of DNS to CLIO or qdots could increase the sensitivity of MR and optical imaging to monitor DNS receptors *in vivo*.

In this study, we examined whether the DNS receptor/probe approach could form the basis of a multimodality imaging system to non-invasively monitor reporter gene expression. Toward this goal, DNS was covalently coupled with CLIO and qdots to form DNS-CLIO and DNS-qdot nanoparticles for MR imaging and optical imaging, respectively. We show that DNS-CLIO and DNS-qdots can selectively accumulate at the DNS receptors *in vitro*. We also show that sites of DNS receptor gene expression can be imaged in animals by MR or optical imaging after intravenous (i.v.) injection of DNS-CLIO or DNS-qdot probes.

Experimental procedures

Reagents

Dansyl chloride and 2,2'-(ethylenedioxy) bis(ethylamine) (EDBE) were from Sigma-Aldrich (St Louis, MO). Dextran T-40 polymer (MW_{av} = 40 000) was from Amersham Biosciences (Piscataway, NJ). Qdot 655 nanocrystals (quantum dots) were from Quantum Dot Corporation (Hayward, CA). B16F1 melanoma and CT26 colon carcinoma cells were from the American Type Culture Collection (Manassas, VA).

Cells and animals

B16/DNS, CT26/DNS, B16/phOx and CT26/phOx cells expressing DNS or phOx receptors, respectively, have been described.^{20,21} Cells were cultured in Dulbecco's minimal essential medium (Sigma, St Louis, MO) supplemented with 10% bovine serum, 100 U ml⁻¹ penicillin and 100 µg ml⁻¹ streptomycin at 37 °C in an atmosphere of 5% CO₂. C57BL/6 and Balb/c mice were obtained from the National Laboratory Animal Center, Taipei, Taiwan. Animal experiments were performed in accordance with institute guidelines.

Synthesis of DNS-CLIO nanoparticles

Synthesis of DNS-EDBE. A solution containing 1 g (3.52 mmol) dansyl chloride and 5.44 ml (35.44 mmol) EDBE in 10 ml toluene was stirred for 60 min at room temperature. The reaction product was purified on silica

gel using the solvent system of dichloromethane:methanol that is equal to 2:8. Purified DNS-EDBE was dried and maintained at 4 °C. MS (ESI) $m/z = 381.2 [M]^+ ^1\text{H-NMR}$ (400 MHz, CDCl₃), δ (p.p.m.): 8.52, 8.36, 8.24–8.21, 7.58–7.53, 7.52–7.48, 7.19–7.15(m, 6H, DNS), 3.58 (t, 2H, -OCH₂CH₂NH-DNS), 3.53–3.50(m, 2H, NH₂CH₂CH₂O-), 3.46–3.43(m, 4H, -OCH₂CH₂O-), 3.11(t, $J = 5.2$, 2H, -OCH₂CH₂NH-), 2.96(t, $J = 5.2$, 2H, NH₂CH₂CH₂O-), 2.88(s, 6H, N (CH₃)₂).

Synthesis of SPIO nanoparticles. Iron oxide particles were prepared by mixing 5 ml of 50% (w/w) dextran T-40 with an equal volume of an aqueous solution containing 0.45 g (2.72 mmol) anhydrous ferric chloride and 0.32 g (1.58 mmol) ferrous chloride tetrahydrate. The mixture was stirred vigorously at room temperature and then 10 ml of 7.5% (v/v) ammonium hydroxide was rapidly added. The black suspension was stirred continuously for 1 h at room temperature and subsequently centrifuged at 17 300 g for 10 min to remove aggregates. The reaction mixture (5 ml) was applied to a 2.5 cm (internal diameter) × 33 cm (length) Sephacryl S-300 column and eluted with buffer solution containing 0.1 M sodium acetate and 0.15 M sodium chloride at pH 6.5 to remove free dextran. The purified iron oxide–dextran particles were assayed for iron at 330 nm and for dextran at 490 nm by the phenol/sulfuric acid method.²² The iron oxide–dextran particles were extensively dialyzed and stored at 4 °C.

Synthesis of CLIO. Five milliliters of iron oxide–dextran particles (7–10 mg ml⁻¹ Fe) were added to a solution containing 3.3 ml (43 mmol) epichlorohydrin and 8.4 ml 5 N sodium hydroxide. After stirring vigorously for 24 h at 25 °C, the solution was dialyzed against five changes of distilled water (2 L each) to obtain CLIO particles.

Synthesis of DNS-CLIO. A total of 0.5 g (13.12 mmol) of dansyl-EDBE (Ex/Em; 455/530 nm) in 1 ml methanol was added to 20 ml CLIO (2 mg ml⁻¹ Fe) and stirred for 24 h at room temperature to form DNS-CLIO nanoparticles. The product was extensively dialyzed in phosphate-buffered saline (PBS) and stored at 4 °C.

Size and fluorescent measurement of DNS-CLIO

The average particle size and morphology of iron oxide particles were examined using a JEOL JEM-2000 EX II transmission electron microscope at a voltage of 100 kV. An aqueous dispersion of the particles was drop-cast onto a carbon-coated copper grid and air-dried before loading into the microscope. Fluorescent measurements were obtained on a FLUOSTAR galaxy (BMG LabTechnologies GmbH, Offenburg, Germany) at 355/530 nm excitation/emission at a concentration of 1 mM iron at room temperature.

Preparation of DNS-qdots

Six micrograms (22.5 nmol) of dansyl chloride in DMF was reacted with 0.25 nmol qdots at a molar ratio of 90:1 in 0.1 M NaHCO₃, pH 8 at room temperature for 1 h to

generate DNS-qdots. DNS-qdots were separated from unreacted dansyl chloride by gel filtration on a Sephadex G-25 column equilibrated with PBS.

Flow cytometer analysis

Specific binding of DNS-CLIO was examined by staining 10^5 B16/DNS cells with $1\ \mu\text{M}$ DNS-fluorescein isothiocyanate (FITC), a mixture of DNS-CLIO ($13.45\ \text{mM Fe}$)/ $1\ \mu\text{M}$ DNS-FITC or PBS at 4°C for 40 min. Similarly, B16/phOx cells were incubated with $1\ \mu\text{M}$ phOx-FITC, DNS-CLIO ($13.45\ \text{mM Fe}$)/ $1\ \mu\text{M}$ phOx-FITC or PBS under the same conditions. The cells were washed twice with cold PBS and the immunofluorescence of 10 000 viable cells was measured on a FACScaliber flow cytometer (Beckman Coulter, Fullerton, CA). Fluorescence intensities were analyzed with Flowjo V3.2 (Tree Star, Inc., San Carlos, CA).

In vitro cytotoxicity of DNS-CLIO

A total of 10^6 CT-26/DNS and 10^6 CT-26/phOx cells were seeded overnight in 96-well microtiter plates before graded concentrations of DNS-CLIO or *p*-hydroxyaniline mustard (pHAM) were added to the cells in triplicate for 24 h at 37°C . The cells were subsequently incubated for 48 h in fresh medium. Cell viability was determined by the ATPlite Luminescence ATP Detection Assay System (ATPlite, Perkin Elmer, Boston, MA). Results are expressed as percent inhibition of luminescence compared with untreated cells.

MR imaging in vitro

B16/DNS and B16/phOx cells (3×10^6 cells) were stained with DNS-CLIO ($7.25\ \text{mM Fe}$) for 30 min on ice. After washing with cold PBS, the DNS-CLIO-labeled cells were mixed with unlabeled cells at defined ratios (100:0, 50:50, 10:90, 0:100) in 0.2 ml tubes; each tube contained 3×10^6 cells. Cells were centrifuged (1000 r.p.m.) and MR imaging was performed with a clinical 3.0-T MR imager (Sigma; GE Medical system, Milwaukee, WI) and a high-resolution head coil. All samples were measured by T2-weighted spin-echo sequences (TR/TE/flip angle = $18/7.3/10^\circ$).

MR imaging in vivo

C57BL/6 mice bearing established B16/phOx and B16/DNS tumors ($200\ \text{mm}^3$) in their left and right shoulder regions, respectively, were i.v. injected with DNS-CLIO ($20\ \mu\text{mol Fe}$ per kg body weight). The whole-body imaging of pentobarbital-anesthetized mice was performed between 0 and 2 h and at 24 h with the use of 7-T horizontal bore magnet (Bruker Biospin GmbH, Ettlingen, Germany). A T2-weighted spin-echo sequence (TR 4000 ms/TE 76 ms) was used for MR imaging.

Fluorescence imaging in vitro and in vivo

A total of 10^6 CT26/DNS and 10^6 CT26/phOx cells were stained with DNS-qdots ($0.125\ \mu\text{M}$) in PBS containing 0.05% BSA at room temperature for 40 min. The cells were washed with cold PBS and examined under a fluorescence microscope. Balb/c mice bearing CT26/phOx

and CT26/DNS tumors ($200\ \text{mm}^3$) in their left and right flanks, respectively, were i.v. injected with 0.11 nmol DNS-qdots. Whole-body images of pentobarbital-anesthetized mice were obtained at 2 h with a charged-coupled device camera (Maestro™ CRI-INC).

Statistical significance

Statistical significance of differences between mean values was estimated with Excel (Microsoft, Redmond, WA) using the independent *t*-test for unequal variances. *P*-values of less than 0.05 were considered to be statistically significant.

Results

Characterization of the DNS-CLIO probe

The reaction of ferrous chloride with ferric chloride under alkaline conditions in the presence of dextran T-40 yielded a suspension of dextran-coated colloidal particles. Figure 1 shows a transmission electron microscopy image of the iron oxide suspension. The mean core size ($n = 200$) of the iron oxide nanoparticles was $10.3 \pm 2.2\ \text{nm}$. In aqueous solution, the relaxivity values (r_1 and r_2) of the iron oxide-dextran particles at 20 MHz, 37°C were 41.2 ± 0.3 and $110.6 \pm 0.4\ \text{mM}^{-1}\ \text{s}^{-1}$, respectively. Dansyl chloride was first linked to EDDB to increase its hydrophilicity and then reacted with CLIO (Scheme 1) to form DNS-CLIO. Figure 2 shows that the fluorescent intensity of the DNS-CLIO particles was significantly higher than that of iron oxide nanoparticles (SPIO) alone, demonstrating that the DNS hapten was successfully linked to CLIO to form the DNS-CLIO MR imaging probe.

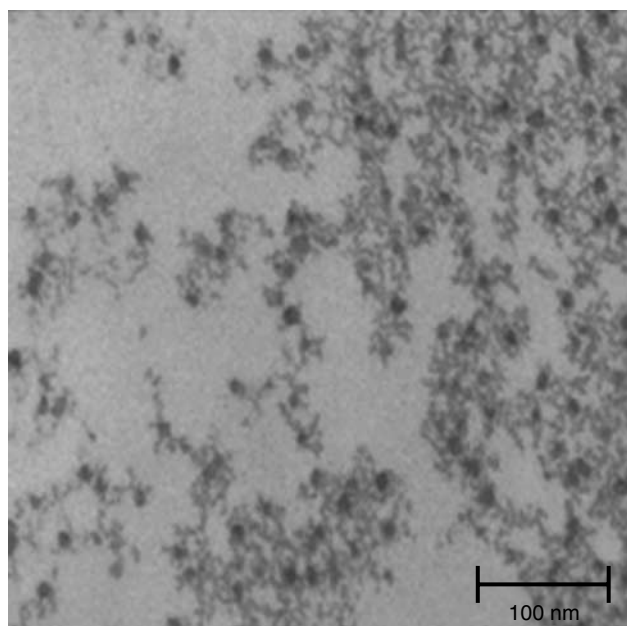
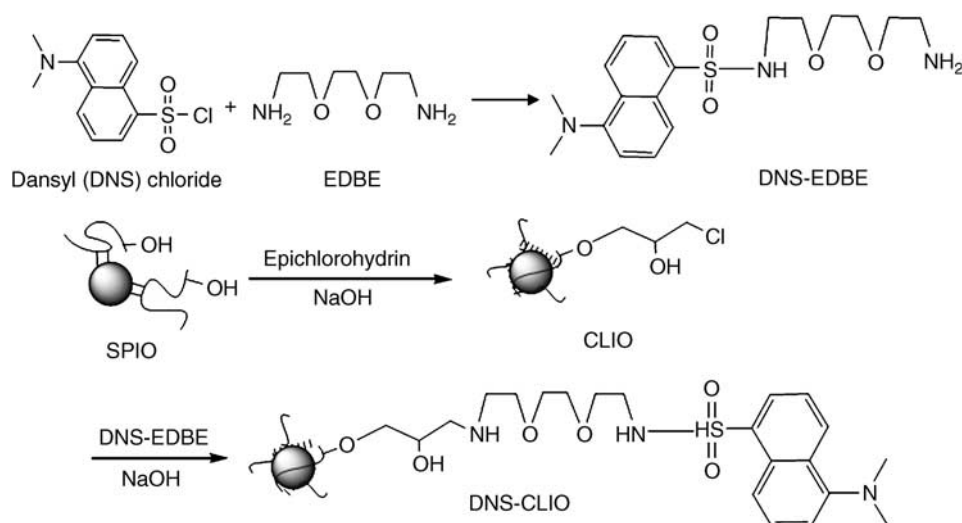


Figure 1 Transmission electron microscopy (TEM) image of iron oxide nanoparticles. The scale bar is 100 nm.



Scheme 1 Synthetic scheme for the DNS-CLIO imaging probe. Dansyl (DNS) chloride was linked to 2,2'-(ethylenedioxy) bis(ethylamine) (EDBE) and then reacted with CLIO nanoparticles to form the DNS-CLIO MR imaging probe.

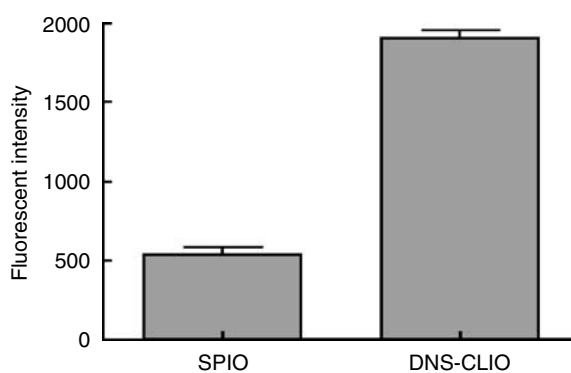


Figure 2 The fluorescent intensity of SPIO and DNS-CLIO probes. The fluorescent intensity of iron oxide-dextran nanoparticles (SPIO) and DNS-cross-linked iron oxide nanoparticles (CLIO) were measured at 355/530 nm (excitation/emission) at a concentration of 1 mM iron at room temperature on a FLUOSTAR galaxy.

The specific binding and cytotoxicity of DNS-CLIO

The specific binding of DNS-CLIO by DNS receptors was examined in a competition assay. DNS-CLIO specifically blocked DNS-FITC binding to B16/DNS cells (Figure 3a) but could not compete the binding of phOx-FITC to B16/phOx cells (Figure 3b), demonstrating that DNS-CLIO specifically bound to DNS receptors but not to control phOx receptors. The cytotoxicity of DNS-CLIO was also investigated by incubating defined concentrations of DNS-CLIO with B16/DNS and B16/phOx cells for 24 h. Figure 4 shows that DNS-CLIO (up to 100 μM Fe) did not inhibit the growth of B16/DNS or B16/phOx cells whereas the positive control (*p*-hydroxyaniline mustard, an alkylating agent) killed the cells. These results show that DNS-CLIO nanoparticles display minimal cytotoxicity to cells expressing DNS or control phOx receptors.

MR imaging of DNS receptors *in vitro* and *in vivo*

To examine DNS-CLIO binding *in vitro*, B16/DNS and B16/phOx cells were incubated with DNS-CLIO (7.25 mM Fe) at 4 °C, washed and then mixed with unlabeled cells at defined ratios. The cells were then analyzed on T2-weighted images in a clinical 3.0 T superconductive MR scanner. Figure 5a shows that mixed populations containing as few as 10% DNS-CLIO-labeled B16/DNS cells but not B16/phOx cells displayed dark areas, a positive T2-weighted signal, in T2-weighted images, indicating selective binding of DNS-CLIO to cells expressing DNS receptors. For *in vivo* non-invasive imaging, C57BL/6 mice bearing established B16/phOx and B16/DNS tumors in their left and right shoulder regions, respectively, were *i.v.* injected with DNS-CLIO (20 μmol Fe per kg body weight). Whole-body images of the mice performed on T2-weighted images in a 7.0 MR scanner show that DNS-CLIO was selectively retained in B16/DNS tumors, leading to a marked reduction of the signal intensity (a positive T2-weighted signal) in B16/DNS tumors but not in control B16/phOx tumors (Figure 5b). The DNS-CLIO-induced reduction of signal intensity in the B16/DNS tumor (Figure 5c) correlated well with T2-weighted MR images of the tumor (Figure 5b). By contrast, B16/phOx tumors did not exhibit reduced signal intensity during MR imaging (Figures 5b and c). These results indicate that DNS-CLIO could selectively monitor DNS receptor location by MR imaging *in vivo*.

Fluorescence imaging of DNS receptors *in vitro* and *in vivo*

DNS-qdots selectively bound CT26/DNS cells but not control CT26/phOx cells (Figure 6a). For non-invasive imaging *in vivo*, mice bearing a control CT26/phOx tumor on their left flank and CT26/DNS tumor on their right flank were *i.v.* injected with 0.11 nmol DNS-qdots. The mice were then imaged with a charged-coupled device

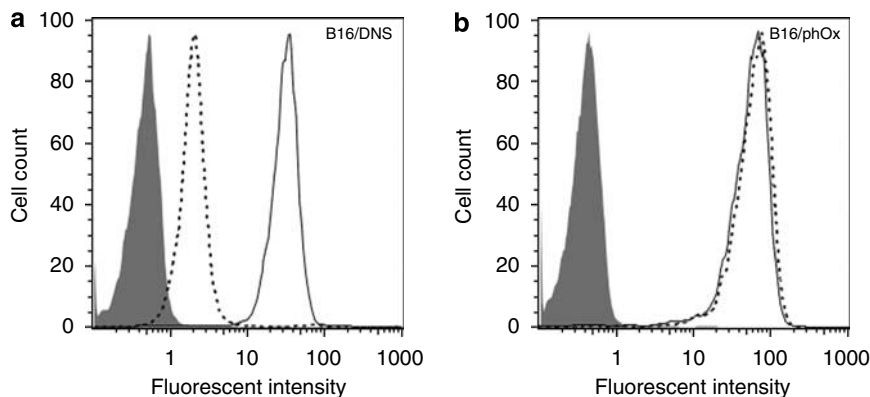


Figure 3 Specific binding of DNS-CLIO to DNS receptors. B16/DNS cells (a) were incubated with $1\ \mu\text{M}$ DNS-fluorescein isothiocyanate (FITC) (solid line), DNS-CLIO ($13.45\ \text{mM Fe}$)/ $1\ \mu\text{M}$ DNS-FITC (dashed line) or phosphate-buffered saline (PBS) (solid curve), respectively. B16/phOx (b) cells were incubated with $1\ \mu\text{M}$ pHx-FITC (solid line), DNS-CLIO ($13.45\ \text{mM Fe}$)/ $1\ \mu\text{M}$ pHx-FITC (dashed line) or PBS (solid curve) under the same conditions. Cells were washed and the surface immunofluorescence of 10000 viable cells was measured with a FACScaliber flow cytometer.

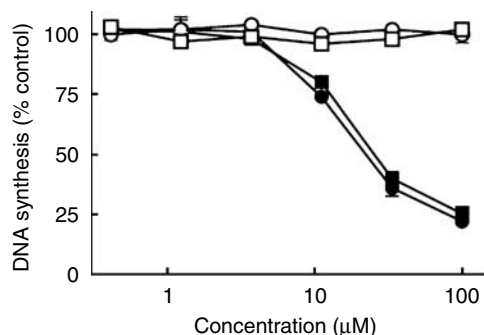


Figure 4 The cytotoxicity of the DNS-CLIO probe. B16/DNS (\circ , \bullet) and B16/phOx (\square , \blacksquare) cells were treated with graded concentrations of DNS-CLIO (\circ , \square) or *p*-hydroxyaniline mustard (pHAM) (\bullet , \blacksquare) for 24 h. Cells were subsequently incubated for 48 h in fresh medium and cell viability was determined by the ATPlite Luminescence ATP Detection Assay System. Results are expressed as percentage inhibition of luminescence compared with untreated cells.

camera after 2 h. Figure 6b shows that DNS-qdots were preferentially retained in CT26/DNS tumors as compared to control CT26/phOx tumors, indicating that DNS-qdots can image sites of DNS receptor expression by optical imaging *in vivo*.

Discussion

We developed a non-invasive imaging system based on the expression of DNS single-chain antibody receptors on cells to trap DNS-derivatized probes. Our results demonstrate that DNS-derivatized-CLIO and qdot nanoparticles are selectively retained at the DNS receptors and can be detected *in vitro* and *in vivo* by MR and optical imaging methods. We previously showed that DNS receptors can specifically trap a bivalent $(\text{DNS})_2$ -dithylenetriaminepentaacetate- ^{111}In ($(\text{DNS})_2$ -DTPA- ^{111}In) probe in mice,

as assessed by gamma camera imaging.¹¹ These results suggest that multimodality imaging (MR, optical and gamma camera imaging) can be employed to monitor DNS receptors *in vivo* by choosing the proper DNS probe.

The specificity and sensitivity of an imaging probe are critical for the successful detection of receptors *in vivo*. We previously showed that DNS-derivatized-DTPA- ^{111}In and DNS-derivatized β -glucuronidase²¹ could localize to DNS receptors on cells *in vitro* and *in vivo*. Similar results were also shown in this study for DNS-derivatized CLIO and qdots. Thus, DNS-derivatized molecules possess sufficient specificity to allow effective targeting to DNS receptors *in vivo*. However, the sensitivity of the $((\text{DNS})_2$ -DTPA-Gd (III)) probe was insufficient to image DNS receptors *in vivo* by MR imaging (unpublished results). Iron oxide nanoparticles allow more sensitive MR detection. For example, Will *et al.* reported that iron oxide nanoparticle-enhanced MR imaging was more sensitive than unenhanced MRI for the detection of lymph-node tumor metastases.²³ Hogemann *et al.* also reported that transferrin-labeled CLIO increased MR sensitivity for the detection of endogenous transferrin receptors.^{12,13} Our results show that a mixture containing less than 10% of DNS-CLIO saturated B16/DNS cells could be detected by MR imaging *in vitro* and targeted DNS-CLIO specifically produced signal changes in B16/DNS tumors *in vivo*. Similar results were also shown for DNS-qdot targeting and imaging of DNS receptors *in vitro* and *in vivo*. These results indicate that DNS-derivatized nanoparticles may be useful as contrast agents and to enhance the sensitivity of MR and optical imaging for monitoring gene expression *in vivo*.

Multivalent binding of probes can enhance avidity for more persistent binding to allow imaging over an extended time window. We previously found that accumulation of a dimeric $(\text{DNS})_2$ -DTPA- ^{111}In probe at DNS receptors *in vivo* was superior as compared to a monomeric DNS-DTPA- ^{111}In probe.¹¹ Similarly, Cortens *et al.* reported increased uptake of a dimeric DTPA- ^{111}In

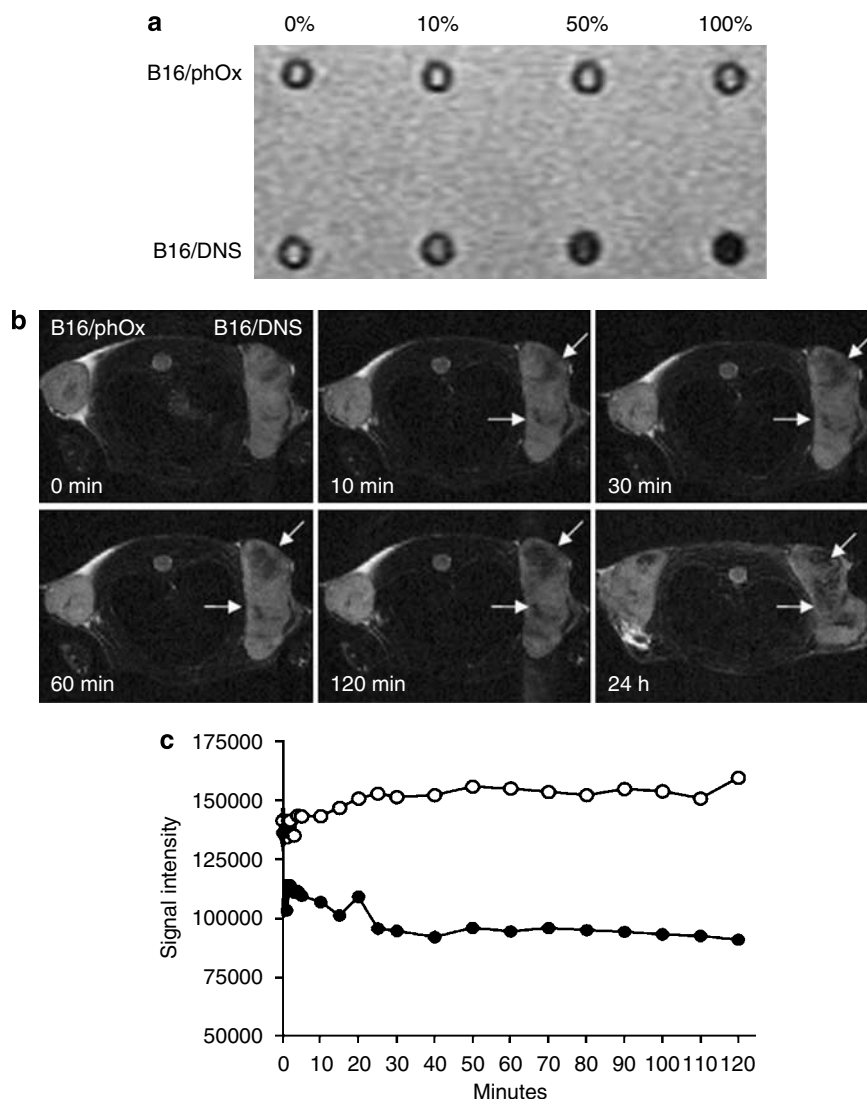


Figure 5 MR imaging of DNS receptors *in vitro* and *in vivo*. **(a)** A total of 3×10^6 B16/phOx (upper panel) or B16/DNS (lower panel) cells were stained with DNS-CLIO, washed with cold PBS and mixed with unlabeled cells at the ratios of 100:0 (100%), 50:50 (50%), 10:90 (10%) or 0:100 (0%). The cells were imaged in a clinical 3.0-T MR imager equipped with a high-resolution head coil. For *in vivo* imaging, DNS-CLIO ($20 \mu\text{mol Fe}$ per kg body weight) was intravenously (i.v.) injected into mice bearing B16/phOx (left side) and B16/DNS (right side) tumors. **(b)** Whole-body images of the mice were performed at the indicated times on T2-weighted images (TR 4000 ms/TE 76 ms) in a 7.0 MR scanner. **(c)** The signal intensities in B16/phOx (○) and B16/DNS (●) tumors were acquired during 0–2 h. The dark areas in the cells and tumors represent positive T2-weighted signals.

probe in a two-step approach for radioimmunotargeting of cancers.^{24,25} Goel *et al.* showed that tetravalent CC49 antibody allowed three times better localization than divalent CC49 in human colon carcinoma.²⁶ These results suggest that multivalent binding is highly desirable to enhance the avidity and reduce off-rate *in vivo*. Recently, multivalent magnetic and fluorescent nanoparticles have become important materials for biological applications.^{27–29} In our study, multivalent DNS-derivatized CLIO and qdot nanoparticles allowed effective targeting to DNS receptors *in vivo*. These results support the notion that multivalent imaging probes may be suited for *in vivo* targeting application.

We did not observe DNS-CLIO toxicity to B16F1 cells expressing DNS or phOx receptors, consistent with low toxicity of DNS-CLIO. Similarly, Hussain *et al.* showed that CLIO/ Fe_3O_4 nanoparticles displayed little toxicity for liver cells³⁰ and Weissleder *et al.* reported that CLIO-labeled CD8^+ T cells remained >95% functionally viable and displayed similar activity as unlabeled cells.³¹ Dextran-coated SPIO nanoparticles have been approved by the Food and Drug Administration as MR contrast agents (ferumoxides, ferumoxtran, ferumoxsil) for use in hepatic reticuloendothelial cell imaging and ultra-small SPIOs (USPIOs) are in phase III clinical trials for use as blood pool agents or for use with lymphography.^{32,33}

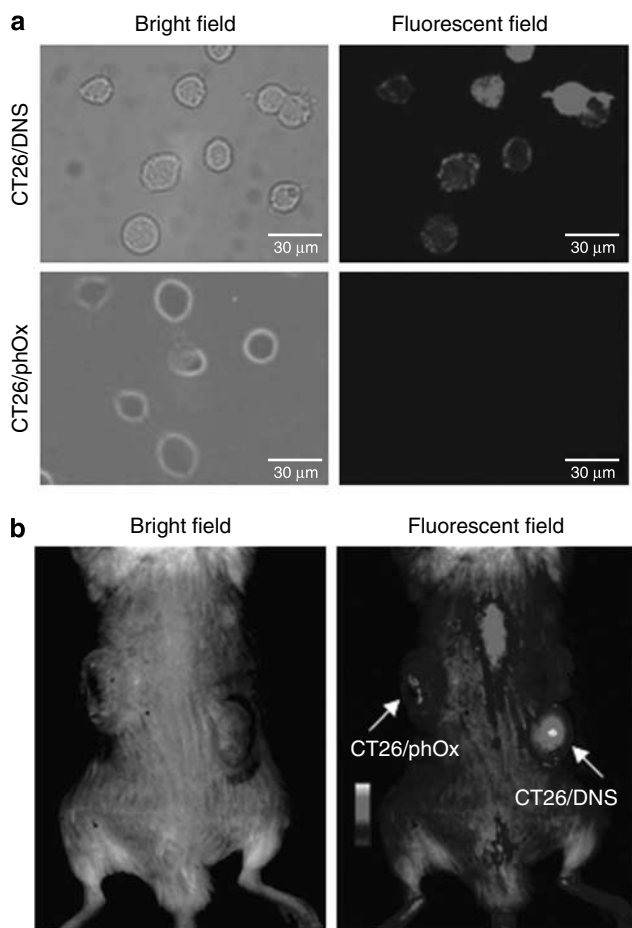


Figure 6 Fluorescence imaging of DNS receptors *in vitro* and *in vivo*. (a) CT26/DNS cells (upper panels) or CT26/phOx cells (lower panel) were stained with DNS-quantum dots (qdots). After washing, the cells were observed under visible or fluorescent light. The scale bar is 30 μm . (b) DNS-qdots were intravenously injected into mice bearing CT26/phOx (left) and CT26/DNS (right) tumors and the whole-body images of pentobarbital-anesthetized mice were obtained at 2 h with a charged-coupled device camera.

Furthermore, DNS receptors derived from a murine immunoglobulin did not induce a detectable antibody response in mice,¹¹ demonstrating that DNS receptors possess low immunogenicity. A human DNS antibody receptor could be employed to maintain low immunogenicity in humans. Based on these results, the DNS probe/DNS receptor system should be suitable for *in vivo* imaging of gene expression in both animals and humans.

Each molecular imaging modality has its own inherent strengths and weaknesses and can be used to address different questions in biomedical research. Development of a multimodality reporter imaging system is important for imaging *in vivo* gene expression. A range of DNS-derivatized contrast agents can be created for imaging DNS receptors. The DNS moiety is a small molecule which has been extensively employed to form derivatives for quantitative analysis of amino acids,³⁴ manual peptide sequencing³⁵ as well as ion and proton detection.³⁶ We previously showed that a (DNS)₂-DTPA-¹¹¹In probe

specifically localized to DNS receptors in mice as assessed by gamma camera imaging.¹¹ Similarly, these results show that DNS can be attached to CLIO or qdot nanoparticles to specifically image DNS receptors *in vitro* and *in vivo* by MR or optical imaging systems. Our studies indicate that DNS can be employed to form MRI contrast agents, SPECT probes and fluorescent probes to monitor gene expression by different imaging modalities, indicating that the DNS receptor/DNS probe system possesses non-invasive multimodality imaging properties that fits many application requirements.

In summary, the advantages of the DNS receptor/DNS probe system for non-invasive imaging include (1) the high specificity of antibody-antigen interactions to allow sensitive detection of probes without interference from cellular factors, (2) the high avidity of multivalent DNS probes allows prolonged retention *in vivo*, (3) the low toxicity of DNS-derivatized probes and low immunogenicity of DNS receptors should minimize tissue damage and immune responses to allow repeated and persistent imaging of gene expression *in vivo* and (4) DNS can be linked to any suitable probe to allow imaging by alternative modalities. Based on these advantages, we believe that the novel DNS probe/DNS receptor system possesses attractive characteristics for monitoring gene expression in live animals and has clinical potential for human gene therapy.

Acknowledgements

This work was supported by the National Research Program for Genomic Medicine (NRPGM), National Science Council, Taipei, Taiwan (NSC95-3112-B-037-001, NSC 95-2627-M-037-001) and the National Health Research Institutes (NHRI-EX96-9624SI). We acknowledge technical support from the Functional and Micro-Magnetic Resonance Imaging Center supported by the National Research Program for Genomic Medicine, National Science Council, Taiwan (NSC95-3112-B-001-009) and the National Sun Yat-Sen University-Kaohsiung Medical University Joint Research Center.

References

- 1 Serganova I, Blasberg R. Reporter gene imaging: potential impact on therapy. *Nucl Med Biol* 2005; **32**: 763–780.
- 2 Juweid ME, Cheson BD. Positron-emission tomography and assessment of cancer therapy. *N Engl J Med* 2006; **354**: 496–507.
- 3 Bell JD, Taylor-Robinson SD. Assessing gene expression *in vivo*: magnetic resonance imaging and spectroscopy. *Gene Ther* 2000; **7**: 1259–1264.
- 4 Louie A. Design and characterization of magnetic resonance imaging gene reporters. *Methods Mol Med* 2006; **124**: 401–417.
- 5 Golzio M, Rols MP, Gabriel B, Teissie J. Optical imaging of *in vivo* gene expression: a critical assessment of the methodology and associated technologies. *Gene Ther* 2004; **11**(Suppl 1): S85–S91.

- 6 Shah K, Weissleder R. Molecular optical imaging: applications leading to the development of present day therapeutics. *NeuroRx* 2005; **2**: 215–225.
- 7 Madsen MT, Park CH. Enhancement of SPECT images by Fourier filtering the projection image set. *J Nucl Med* 1985; **26**: 395–402.
- 8 Weissleder R, Ntziachristos V. Shedding light onto live molecular targets. *Nat Med* 2003; **9**: 123–128.
- 9 Delikatny EJ, Poptani H. MR techniques for *in vivo* molecular and cellular imaging. *Radiol Clin North Am* 2005; **43**: 205–220.
- 10 Yeung HW, Macapinlac H, Karpel M, Finn RD, Larson SM. Accuracy of FDG-PET in gastric cancer. Preliminary experience. *Clin Positron Imaging* 1998; **1**: 213–221.
- 11 Roffler SR, Wang HE, Yu HM, Chang WD, Cheng CM, Lu YL *et al*. A membrane antibody receptor for noninvasive imaging of gene expression. *Gene Ther* 2006; **13**: 412–420.
- 12 Hogemann D, Josephson L, Weissleder R, Basilion JP. Improvement of MRI probes to allow efficient detection of gene expression. *Bioconjug Chem* 2000; **11**: 941–946.
- 13 Hogemann-Savellano D, Bos E, Blondet C, Sato F, Abe T, Josephson L *et al*. The transferrin receptor: a potential molecular imaging marker for human cancer. *Neoplasia* 2003; **5**: 495–506.
- 14 Moore A, Sun PZ, Cory D, Hogemann D, Weissleder R, Lipes MA. MRI of insulinitis in autoimmune diabetes. *Magn Reson Med* 2002; **47**: 751–758.
- 15 Anderson SA, Shukaliak-Quandt J, Jordan EK, Arbab AS, Martin R, McFarland H *et al*. Magnetic resonance imaging of labeled T-cells in a mouse model of multiple sclerosis. *Ann Neurol* 2004; **55**: 654–659.
- 16 Gao X, Cui Y, Levenson RM, Chung LW, Nie S. *In vivo* cancer targeting and imaging with semiconductor quantum dots. *Nat Biotechnol* 2004; **22**: 969–976.
- 17 Portney NG, Ozkan M. Nano-oncology: drug delivery, imaging, and sensing. *Anal Bioanal Chem* 2006; **384**: 620–630.
- 18 Rotomskis R, Streckyte G, Karabanovas V. [Nanoparticles in diagnostics and therapy: towards nanomedicine]. *Medicina (Kaunas)* 2006; **42**: 542–558.
- 19 Pinaud F, Michalet X, Bentolila LA, Tsay JM, Doose S, Li JJ *et al*. Advances in fluorescence imaging with quantum dot bio-probes. *Biomaterials* 2006; **27**: 1679–1687.
- 20 Cheng TL, Liao KW, Tzou SC, Cheng CM, Chen BM, Roffler SR. Hapten-directed targeting to single-chain antibody receptors. *Cancer Gene Ther* 2004; **11**: 380–388.
- 21 Chuang KH, Cheng CM, Roffler SR, Lu YL, Lin SR, Wang JY *et al*. Combination cancer therapy by hapten-targeted prodrug-activating enzymes and cytokines. *Bioconjug Chem* 2006; **17**: 707–714.
- 22 Molday RS, MacKenzie D. Immunospecific ferromagnetic iron-dextran reagents for the labeling and magnetic separation of cells. *J Immunol Methods* 1982; **52**: 353–367.
- 23 Will O, Purkayastha S, Chan C, Athanasiou T, Darzi AW, Gedroyc W *et al*. Diagnostic precision of nanoparticle-enhanced MRI for lymph-node metastases: a meta-analysis. *Lancet Oncol* 2006; **7**: 52–60.
- 24 Boerman OC, Kranenborg MH, Oosterwijk E, Griffiths GL, McBride WJ, Oyen WJ *et al*. Pretargeting of renal cell carcinoma: improved tumor targeting with a bivalent chelate. *Cancer Res* 1999; **59**: 4400–4405.
- 25 Kranenborg MH, Boerman OC, Oosterwijk-Wakka JC, de Weijert MC, Corstens FH, Oosterwijk E. Development and characterization of anti-renal cell carcinoma x antic-helate bispecific monoclonal antibodies for two-phase targeting of renal cell carcinoma. *Cancer Res* 1995; **55**: 5864s–5867s.
- 26 Goel A, Baranowska-Kortylewicz J, Hinrichs SH, Wisecarver J, Pavlinkova G, Augustine S *et al*. 99mTc-labeled divalent and tetravalent CC49 single-chain Fv's: novel imaging agents for rapid *in vivo* localization of human colon carcinoma. *J Nucl Med* 2001; **42**: 1519–1527.
- 27 Thorek DL, Chen AK, Czupryna J, Tsourkas A. Superparamagnetic iron oxide nanoparticle probes for molecular imaging. *Ann Biomed Eng* 2006; **34**: 23–38.
- 28 Santra S, Dutta D, Walter GA, Moudgil BM. Fluorescent nanoparticle probes for cancer imaging. *Technol Cancer Res Treat* 2005; **4**: 593–602.
- 29 Sun EY, Josephson L, Kelly KA, Weissleder R. Development of nanoparticle libraries for biosensing. *Bioconjug Chem* 2006; **17**: 109–113.
- 30 Hussain SM, Hess KL, Gearhart JM, Geiss KT, Schlager JJ. *In vitro* toxicity of nanoparticles in BRL 3A rat liver cells. *Toxicol In Vitro* 2005; **19**: 975–983.
- 31 Kircher MF, Allport JR, Graves EE, Love V, Josephson L, Lichtman AH *et al*. *In vivo* high resolution three-dimensional imaging of antigen-specific cytotoxic T-lymphocyte trafficking to tumors. *Cancer Res* 2003; **63**: 6838–6846.
- 32 Harisinghani MG, Saini S, Weissleder R, Hahn PF, Yantiss RK, Tempny C *et al*. MR lymphangiography using ultrasmall superparamagnetic iron oxide in patients with primary abdominal and pelvic malignancies: radiographic-pathologic correlation. *AJR Am J Roentgenol* 1999; **172**: 1347–1351.
- 33 Semelka RC, Helmberger TK. Contrast agents for MR imaging of the liver. *Radiology* 2001; **218**: 27–38.
- 34 Bhushan R, Reddy GP. Thin layer chromatography of dansyl and dinitrophenyl derivatives of amino acids. A review. *Biomed Chromatogr* 1989; **3**: 233–240.
- 35 Walker JM. The Dansyl-Edman method for manual peptide sequencing. *Methods Mol Biol* 1997; **64**: 183–187.
- 36 O'Connor NA, Sakata ST, Zhu H, Shea KJ. Chemically modified dansyl probes: a fluorescent diagnostic for ion and proton detection in solution and in polymers. *Org Lett* 2006; **8**: 1581–1584.